Improving the quality of barrier/seed interface by optimizing physical vapor deposition of Cu Film in hollow cathode magnetron

A. Dulkin, E. Ko, L. Wu, I. Karim, K. Leeser, K. J. Park, L. Meng, and D. N. Ruzic

Articles you may be interested in

Improving the quality of barrier/seed interface by optimizing physical vapor deposition of Cu Film in hollow cathode magnetron

A. Dulkin,[a] E. Ko, L. Wu, I. Karim, K. Leeser, and K. J. Park
Novellus Systems Inc., 3940 N. First Street, San Jose, California 95134

L. Meng and D. N. Ruzic
Department of Nuclear, Plasma, and Radiological Engineering, Center for Plasma-Material Interactions, University of Illinois at Urbana-Champaign, Urbana, Illinois 61801

The quality of physical vapor deposition (PVD) grown barrier/seed interface in Cu interconnect metallization was significantly improved by enhancing Cu nucleation on the Ta barrier surface. This was accomplished through filtering of nonenergetic species from the deposition flux, increasing the fraction of Cu ions, improving metal ion flux uniformity, and minimizing gas ion bombardment of the growing film. The self-sputtering ability of Cu was combined with a magnetically confined high-density plasma in the Novellus hollow cathode magnetron (HCM®) PVD source. Spatial profiles of plasma density and temperature, as well as ion flux, metal ion fraction, and ion energy, were measured by planar Langmuir probes, quartz crystal microbalances, and gridded energy analyzers, all located at the wafer level. Multiple criteria, such as seed step coverage and roughness, the seed layer's resistance to agglomeration, and its stability in the plating bath, have been used to evaluate interface quality. As a result, a new and improved Cu PVD process which demonstrates superior stability during subsequent process steps and ensures successful electrofill performance with a more than 50 % reduction in minimal requirement of field thickness as well as sidewall thickness has been developed. © *2011 American Vacuum Society.*
[DOI: 10.1116/1.3602079]

I. INTRODUCTION

The state-of-the-art inter-level metallization process in ultra large scale integration (ULSI) manufacturing employs the damascene process in which Cu lines are inlaid in the previously etched trenches and vias in the dielectric layers.[1] A diffusion barrier commonly consisting a TaN/Ta bilayer and a Cu seed layer is first deposited by physical vapor deposition (PVD). Cu lines are then formed by electroplating on the barrier and seed layers. The reliability of the interconnect metallization depends on the quality of different interfaces, especially on the barrier/seed interface.[2,3] Continuous seed coverage inside the recessed features with good adhesion to the barrier is critical to prevent void formation during electroplating, post-CMP (chemical mechanical planarization) defects, and stress/electromigration failures.

The further shrink of critical dimensions and increase of aspect ratios lead to a challenge for PVD to form an extremely thin seed layer with a high-quality barrier/seed interface. Several factors which are inherent to the PVD process complicate this task. The neutral deposition flux has a wide angular distribution resulting in deposition build-up on the feature corners called overhang, which shadows the sidewall leading to poor step coverage. The thin sidewall film tends to be discontinuous due to island formation during the film growth.[4] Ta and Cu are immiscible metals with respect to each other and do not form alloys at any temperature, which makes Ta(N) a good diffusion barrier for Cu. At the same time the absence of chemical bonds makes the wetting of Cu on Ta difficult.[5] The resulting rough film can be easily attacked by electrolytes during the initiation phase in the plating bath, leading to seed dissolution and subsequent plating voids. Efforts are being made to tackle these difficulties. For example, to increase nucleation density and avoid seed agglomeration, Cu deposition on a Ta underlayer is usually conducted at low temperatures to minimize adatom mobility. The key factor in building a stable film; however, is the presence of energetic metal species in the deposition flux. It had been demonstrated that Cu forms a much stronger interface with the barrier for sputter-deposited films compared to evaporated films.[6] Sputtered Cu atoms leave the target with relatively high energy (a few eV) but lose it rapidly due to collisions with the background gas.[7] The fraction of Cu^+ ions, usually relatively low in the deposition flux, is a very important component. The ions are accelerated by the wafer sheath potential, and thus can increase the nucleation density and adhesion of Cu to Ta due to their surface penetration. Also, the sheath electric field gives high directionality to the ion flux, thereby allowing for a much better step coverage compared to neutral only flux.

A number of techniques have been implemented to increase the ionization of depositing metal species via increased plasma density in magnetron PVD sources, e.g., ionized PVD (iPVD).[8–10] They are mainly based on (1) increasing the power density in the target area by increasing magnetic confinement, (2) applying short high power pulses, and/or (3) supplying additional RF or microwave power to the discharge. Among these techniques, the high power pulsed magnetron has an inherent shortcoming of low deposition rate due to its duty cycle. Utilizing an inductively coupled plasma

(ICP), up to 40 % of Cu atoms in the sputtered flux can be ionized, but the sputtered atoms have to be slowed down through thermalization for effective ionization to occur.[8] The remaining deposition flux is then comprised of slow neutral atoms, similar to those in evaporation systems. To achieve more ionization while maintaining high deposition rate and energetic neutrals, a hollow cathode magnetron (HCM) is used in the present study. It features a unique strong magnetic field confinement of the plasma within the 3-D target geometry, and enhances ionization without a secondary plasma source achieving a high plasma density up to 10^{13} cm^{-3}.[11,12]

The main subject of this paper is improving the quality of barrier/seed interface by optimizing the seed deposition process in the HCM source. This allows the system to handle aggressive-feature geometries associated with the transition to advanced design nodes in ULSI manufacturing. For example, less than 100 nm pitch trenches have been used for 32 nm node. For these applications, an extremely thin sidewall seed with minimal overhang has to be used for successful electrofill. Consequently, the current seed deposition process needs to be optimized so that the very thin seed layer will remain continuous and stable to ensure void-free electroplating and reliability in subsequent process steps. The issues of seed continuity, adhesion and stability were addressed via control of the species and their energies in the deposition flux. The formed seed layers were subjected to cross-sectional scanning electron microscope (SEM) characterization and other indirect quality tests. Special attention was paid to achieving the desirable quality consistently across the entire wafer. The extreme points of the wafer center and edge were typically chosen for comparison taking account that the film characteristics basically change monotonically along the radial direction in this HCM source. Plasma parameters and deposition fluxes, as well as their spatial distributions, have been measured at the wafer level to assist with the process development.

II. EXPERIMENTAL DETAILS

The experiments have been conducted on a Novellus 300 mm INOVA® HCM Cu PVD source which has been described elsewhere.[11] A schematic diagram of the source is presented in Fig. 1. One of the critical distinguishing characteristics of the source is its magnetic field. It exists not only in the source area, as in standard planar magnetrons, but also in the wafer area.[11] By using an unbalanced magnetron configuration, a magnetic separatrix is generated between the target and the substrate. The boundary separates these two regions, allowing to a certain extent independent manipulation of the sputtering plasma at the target and the depositing plasma at the wafer level.

The baseline deposition process used a magnetic field optimized for target utilization and film thickness uniformity while maintaining a high level of Cu ionization for good step coverage. Despite a relatively low Ar pressure of 0.5 mTorr, the electron confinement in the source was very effective. The exponent n in the source current-voltage characteristic
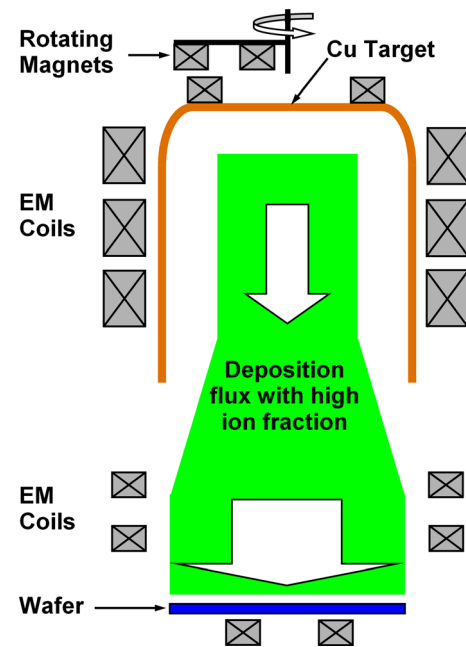
FIG. 1. (Color online) Schematic diagram of the Novellus HCM source. Multiple sets of electromagnetic (EM) coils are used to manipulate the magnetic field and thus control the plasma at the target and the wafer level to a certain degree independently.

$$I = kV^n \tag{1}$$

was measured at 22, which was higher than typical magnetron sputtering values (between 3 and 15). The higher the value n, the more efficient is the electron trapping. Lower values are found when operating at low pressures or by using a weak magnetic field.[8]

The baseline process was modified in a number of aspects. First of all, the magnetic field at the target was manipulated to modulate the target sputtering area. Specifically, the erosion groove was shifted upwards in the source, as shown in Fig. 2. This helps filter out species having low deposition angles with respect to the plane of the wafer by the combination of long throw and collimation effects. Second, a high plasma density was maintained by tight magnetic confinement of the erosion area and thus an increased DC power density. The very high plasma density ($>10^{13}$ cm^{-3}) inside the source makes electron impact the dominant ionization mechanism for metal species.[9] This can reduce the fraction of low energy atoms in the deposition flux, since slower atoms spend more time in the plasma, increasing their chances of getting ionized via electron impact. Third, the Cu self-sputtering was enhanced by the high plasma density and low Ar gas pressure. The high self-sputtering ability of Cu makes it possible to have an ionized flux of Cu species depositing on the wafer with minimum gas ion bombardment.[13] Self-sputtering conditions were achieved by igniting the discharge at <1 mTorr (0.133 Pa) of Ar and immediately reducing the pressure to <0.1 mTorr (0.0133 Pa) upon ignition. At these pressures, there is no thermalization of the sputtered Cu atoms since they travel to the wafer virtually collision-free, so the neutral component of the depositing flux is more energetic compared to the baseline process. Even at such low pressures the exponent n in Eq. (1)
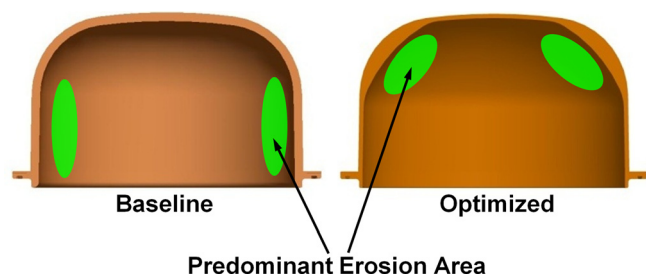
FIG. 2. (Color online) Erosion grooves of the baseline and optimized sputtering processes. Long throw and collimation effects are utilized to improve the deposition angle of sputtered fluxes.

was still about 14 when the DC power was high (55–70 kW), indicating an effective electron confinement in the plasma. Last, the downstream magnetic fields were adjusted to improve the ion flux uniformity. Sputtered Cu atoms can be ionized inside the HCM source close to the target, or in the second area of high plasma density located below the separatrix center, where a magnetic null (zero magnetic field) is formed.[8] A plasma beam escapes from the source through the magnetic null to the wafer following the magnetic field lines created by downstream magnets. The interaction of the source and downstream magnetic fields shapes the separatrix, affecting both the plasma density and beam profile.

Several analytical techniques can be used to measure plasma and flux parameters in the deposition chamber. We have chosen the ones which allowed us to do the measurements at the substrate level. A complex analytical module consisting of planar Langmuir probes, quartz crystal microbalances (QCM), and gridded energy analyzers (GEA) was developed and used to help optimize the deposition process. The Langmuir probe array consisted of 24 planar probes. A spatial resolution of 37.5 mm was achieved by arranging 9 probes along a 300 mm diameter. The QCM/GEA assembly was 75 mm apart from each other along the diameter, located at the center, half radius, and edge of the module. The details of the analytical module construction and operation were discussed elsewhere.[14] The planar Langmuir probes have been used to measure electron density and temperature, ion density, and plasma and floating potentials, from which the ion energy was estimated. QCM and GEA measured the ionization fraction of Cu flux, Cu^+/Ar^+ ratio, and ion energy distribution.

For the barrier/seed deposition comparison between the baseline and the optimized processes, patterned wafers produced by the Novellus Customer Integration Center, as well as commercially-available wafers from IBM were used. We evaluated the barrier/seed interface quality using multiple criteria. The emphasis was placed on the study of the film inside the recessed features, particularly on the sidewalls, where electroplating and reliability problems occur. The film forming fluxes to the recessed feature sidewalls are very different from those to the horizontal surfaces. The common techniques for film characterization have generally been developed for flat, relatively large surfaces. We therefore had to employ indirect and/or qualitative techniques for feature sidewall film characterization. The most important metric was void-free electrofilling of high aspect ratio vias with minimal seed thickness. The plating

bath is a hostile environment for the seed since it will quickly dissolve in the bath if the initiation of plating is delayed. We consequently used the time for which the seed could survive in the bath before plating began as a metric for seed quality. It is well known that even a thick seed on the sidewalls will not ensure void-free plating if the film is not continuous. Film continuity can be gauged by its roughness. Rough films usually form when the nucleation density is low and the growth occurs predominantly by island coalescence mechanism, which leaves behind open areas until the film is relatively thick, usually more than 5–10 monolayers. It is difficult to measure film roughness on the sidewalls of small vias, so we used cross-sectional SEM images for visual analysis of film smoothness. Evaluation of film adhesion was done by annealing the thin sidewall film for 90 s at 300 °C in a hydrogen atmosphere. The degree of subsequent film agglomeration was used as a measure of seed stability.
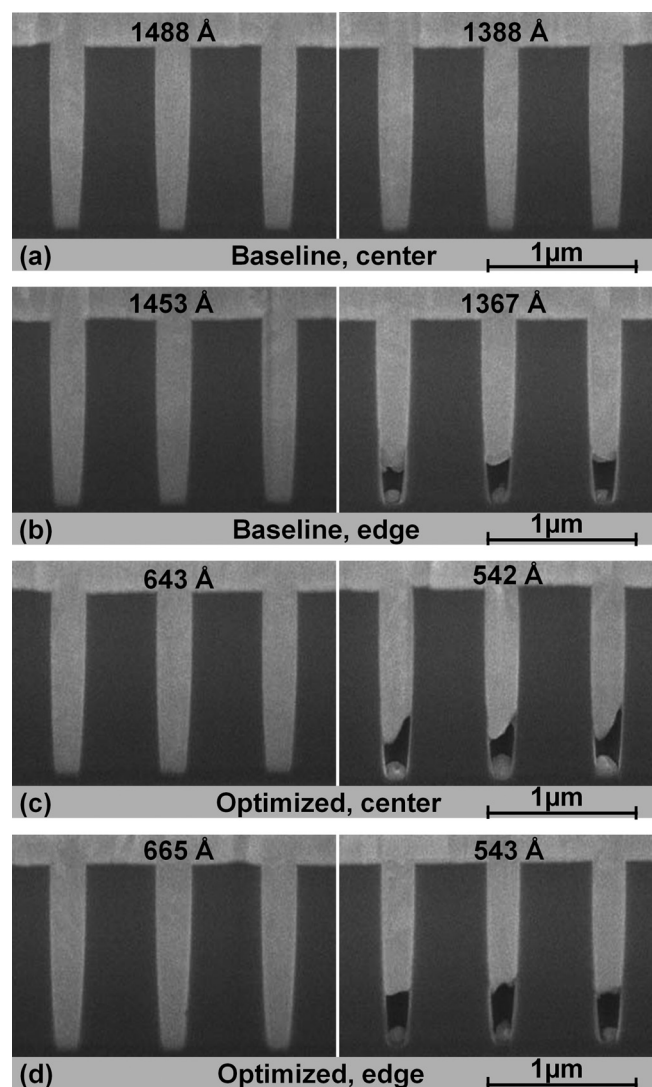

FIG. 3. Electroplating results of 6:1 AR vias with different field thicknesses. (a) and (b) correspond to the baseline Cu seed process at the center and the edge of the wafer, respectively, while (c) and (d) correspond to the optimized process. Please note that the seed deposition layers are not fully displayed in the SEM images. The actual field thicknesses are marked in each image.
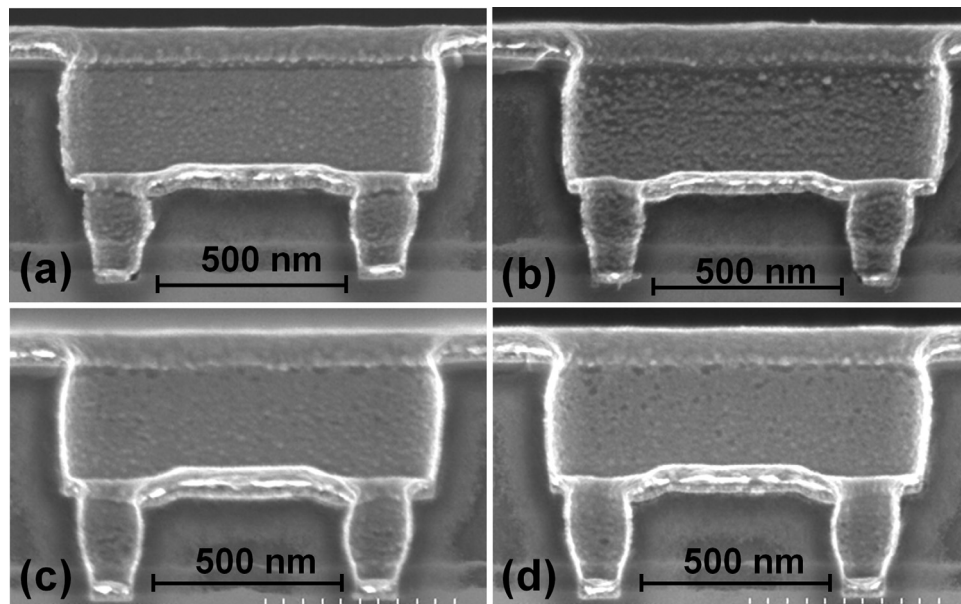
FIG. 4. SEM micrographs of annealed seeds on the via and trench sidewall for the baseline process at the (a) center and (b) edge of the wafer, and for the optimized process at the (c) center and (d) edge.

III. RESULTS AND DISCUSSION

The optimized seed process was evaluated using the above-mentioned techniques and compared with the baseline process, as well as with some modified processes to de-convolute the impact of different factors. To isolate the film thickness effect, we deposited the same amount of material on the sidewalls with both processes, except for the electroplating tests in vias described in the next paragraph. According to transmission electron microscope (TEM) measurements the sidewall coverage was similar between the baseline and optimized processes while the bottom coverage of the optimized process improved significantly, up to 70 % for high aspect ratio vias, likely due to the more directional deposition flux.

High aspect ratio (AR = 6:1) vias of 250 nm were seeded with different field thicknesses using the two processes, and subsequently electroplated. The corresponding SEM micrographs of focused ion beam (FIB) cross-sections are presented in Fig. 3. As mentioned above, the sidewall coverage is similar for the baseline and optimized processes, so the comparison of the sidewall seed thicknesses can be approximately made from the field thicknesses. The minimum field thickness required for void-free fill for the baseline process was about 1450 Å, according to Figs. 3(a) and 3(b). At a reduced field thickness of 1367 Å, voids were observed at the edge of the wafer. The threshold thicknesses for the optimized process at the wafer center and edge were between 550 Å and 650 Å [Figs. 3(c) and 3(d)], reduced by more than 50 %. Voids appeared simultaneously at the center and edge, exhibiting a better uniformity of deposition across the wafer. With the similar sidewall coverage, it can be determined that the minimum sidewall seed thickness required by the optimized process for a successful electrofill was reduced by about a half. The optimized process is thus more viable for the next device generations. As the feature dimensions decrease, it will be more difficult for the baseline process to

deposit the required thick seeds on the sidewall without severe overhang issues. An increase of the preplating aspect ratio after the metallization also presents challenges for the subsequent plating process, especially for the baseline process requiring a larger field thickness.

The adhesion and stability of the seed was evaluated by the degree of film agglomeration after an annealing for 90 s at 300 °C in hydrogen. The cross-sectional SEM images of the seed film on the sidewalls of the trench and via are shown in Fig. 4. A degraded seed quality after the annealing at the wafer edge for the baseline process was observed showing severely agglomerated seed [Fig. 4(b)]. On the
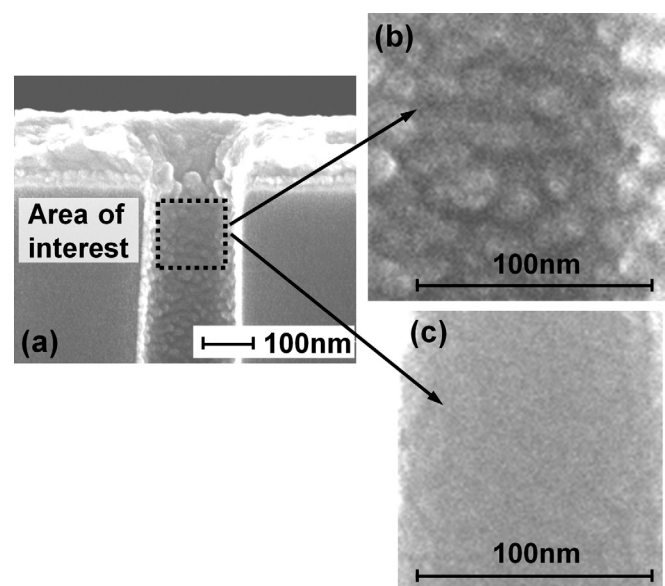

FIG. 5. (a) SEM micrograph of Cu seed on the sidewall of the via structure and the blowup images of the Cu film for the (b) baseline and (c) optimized processes, from the area roughly defined by the dashed rectangle.

contrary the optimized seed resistance to agglomeration was achieved similarly at the wafer center and at the edge (Figs. 4(c) and 4(d)), which again confirmed the improved uniformity of the sidewall film formation by the optimized process as noticed in the previous via electrofill tests.

With the same field thickness of the seed deposition, the optimized seed formed a more continuous layer than the baseline seed as confirmed from SEM images of via sidewall seed roughness in Fig. 5. The baseline process formed a rough film with distinctive grains while the optimized process yielded a much smoother film with weakly defined grain boundaries, as shown in Figs. 5(b) and 5(c), respectively. This proves that nucleation density was increased, explaining how continuous coverage with void-free electroplating was achieved with much less film thickness as in Fig. 3. As mentioned before, low deposition temperatures are usually required to enhance Cu nucleation. We nevertheless were able to deposit the films at a higher temperature (pedestal temperature +20 °C compared to the usual −40 °C) without any detectable degradation in the roughness, continuity, or fill performance using the optimized process. In conjunction with the above hydrogen annealing tests, the superiority of the optimized process with respect to film adhesion and interface stability is evident.

Seed stability was also evaluated with "cold" plating tests, where seeded wafers were subjected to an intentional delay (4 or 6 s) in the plating bath before plating was initiated. The thinnest area of the film deposited by PVD is usually at the middle of a high AR via sidewall. Rough films with well-defined grain boundaries as in Fig. 5(b) were more
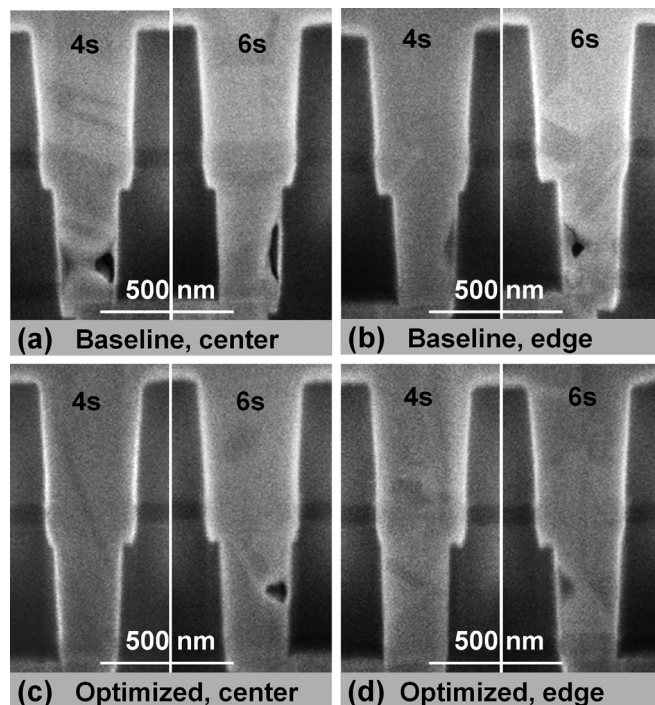

FIG. 6. FIB-SEM cross-sections of "cold" electroplated dual damascene structures with delay times of 4 s and 6 s for the baseline process at the (a) center and (b) edge of the wafer, and for the optimized process at the (c) center and (d) edge.
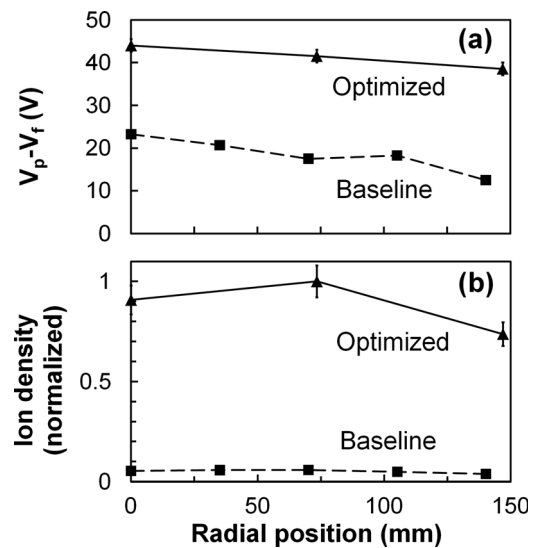
FIG. 7. Radial distribution of the (a) sheath potential drop (V_p-V_f) and (b) ion density across the 300 mm wafer for the baseline and optimized processes. The ion densities were normalized to the max value in the optimized process.

prone to be dissolved faster than smooth ones, like that shown in Fig. 5(c). As soon as the film became discontinuous, a void formed in the mid-sidewall area during subsequent electroplating, as revealed in the FIB-SEM cross-sectional images of electroplated dual damascene structures in Fig. 6. Based on repeated tests, the optimized seed withstood approximately 50 % longer exposure to the "cold" bath than the baseline seed.

We have attributed the improvement in the Cu seed film characteristics to the changes in the deposition flux composition and energies of the species forming the film. This assumption is confirmed by the data obtained with the
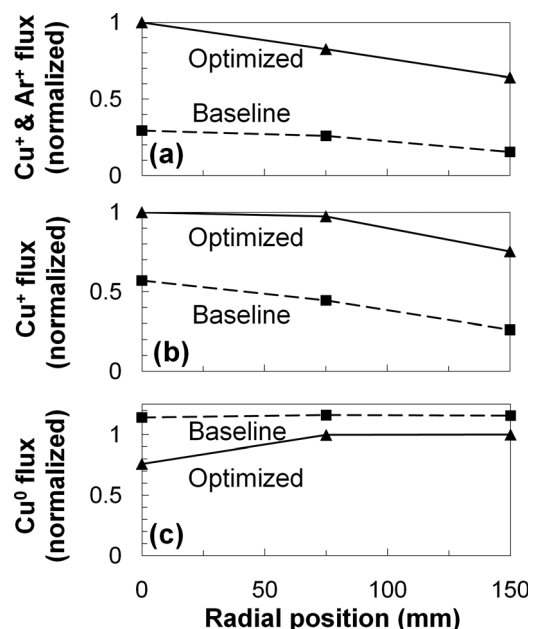

FIG. 8. Radial distribution of (a) total ion of Ar^+ and Cu^+, (b) Cu^+, and (c) Cu^0 in the deposition flux for the baseline and optimized processes.
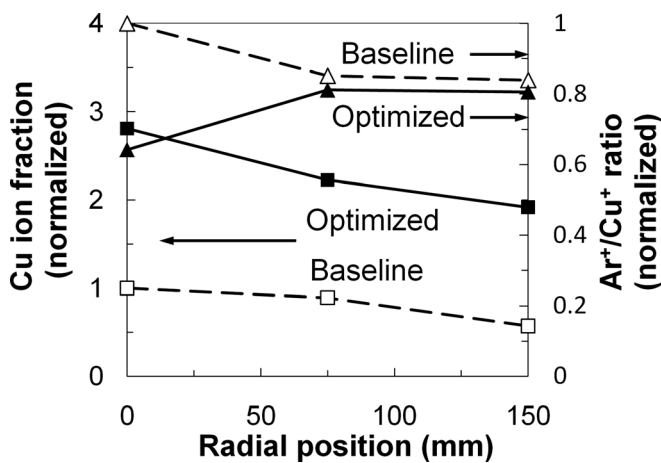
FIG. 9. Radial distribution of (a) Cu ionization fraction and (b) Ar^+/Cu^+ ratio for the baseline and optimized processes.

plasma diagnostic module which was placed inside the deposition chamber in place of a regular wafer.

The plasma sheath potential drop (V_p-V_f), defined as the difference between the plasma potential (V_p) and floating potential (V_{-f}), and the ion density were measured by the Langmuir probe. As shown in Fig. 7(a), the ion energy, which is proportional to the sheath potential, almost doubled for the optimized process and its distribution across the wafer improved. The ion densities, which were normalized to the max value of the optimized process, increased by almost an order of magnitude (Fig. 7(b)). The ion energy distribution measured by the GEA was in good agreement with the Langmuir probe measurements.[14]

A significant change has been observed in the flux composition between the baseline and optimized processes as measured by the QCM/GEA. Figure 8 showed that the total ion flux (Ar^+ and Cu^+) and the Cu^+ flux were increased by two or three times in the optimized process, while the Cu neutral (Cu^0) flux was reduced. Each flux is presented in the form of being normalized to the maximum of corresponding flux in optimized process. The ionization fraction of Cu increased more than two-fold as shown in Fig. 9. While the flux of the baseline process was dominated by Cu neutrals, the optimized process had comparable fluxes of Cu ions and neutrals impinging on the wafer. The Ar^+/Cu^+ ion ratio decreased slightly, which was due to the enhanced Cu self-sputtering effect. It should be noted that the Cu ionization fraction and Ar^+/Cu^+ ion ratio have been normalized to the corresponding maximum value in the baseline process. This higher flux of Cu ions was responsible for the increased nucleation density and adhesion of Cu to Ta with their surface penetration, achieving higher quality seed formation with the optimized process.

IV. CONCLUSIONS

From the film characterizations inside the recessed features and the plasma/deposition flux measurements, we conclude that the critical factors for forming a thin, continuous, and stable Cu seed layer on a Ta underlayer are the amount and distribution of energetic Cu species in the deposition flux. While the high concentration of the energetic Cu

species aids in growing films with better interface qualities, their uniform distribution across the substrate ensures the benefit is not localized to a small area.

We were able to filter out the low energy Cu species from the deposition flux and increase its metal ion fraction by simply changing the magnetic field topology in the HCM source and switching from a gas discharge to essentially a metal discharge plasma. The long throw and collimation effects of the HCM target geometry and the increased power density resulted in a deposition flux dominated by energetic neutrals and metal ions with increased energy. The improved plasma uniformity due to changes in the magnetic field topology at the wafer level led to uniform seed performance across the wafer.

It was shown that there was a significant improvement in the film quality when it was predominantly grown from energetic Cu species. The optimized seed layer agglomerated less when subjected to annealing in hydrogen, did not degrade when deposited at an elevated temperature, was able to withstand a longer delay time during electroplating, and ensured void-free electrofill performance at half the thickness of what was required for the baseline seed. The latter is particularly important for small feature sizes, since overhang limits the maximum seed thickness.

As a result, copper interconnect metallization with a PVD seed layer is facilitated by enabling the formation of very thin but continuous films on the feature sidewalls, and can be extended to the next device generations.

[1]S. Wolf, *Silicon Processing for the VLSI Era, Volume 4: Deep Submicron Process Technology* (Lattice Press, Sunset Beach, 2002).
[2]M. Y. Yan, K. N. Tu, A. V. Vairagar, S. G. Mhaisalkar, and A. Krishnamoorthy, Appl. Phys. Lett. **87**, 261906 (2005).
[3]K. Ishikawa, T. Iwasaki, T. Fujii, N. Nakajima, M. Miyauchi, T. Ohshima, J. Noguchi, H. Aoki, and T. Saito, Proceedings of the IEEE 2003 International Interconnect Technology Conference, Burlingame, CA (IEEE, Piscataway, NJ, 2003), p. 24.
[4]H. Lüth, *Solid Surfaces, Interfaces and Thin Films*, (Springer, 4th Edition, New York, 2001), pp. 100–103.
[5]K. V. Srikrishnan, G. C. Schwartz, *Handbook of Semiconductor Interconnection Technology*, edited by G. C. Schwartz and K. V. Srikrishnan, 2nd ed. (CRC Press, Boca Raton, 2006), pp. 321–325.
[6]S. Kamiya, S. Suzuki, K. Yamanobe, and M. Saka, J. Appl. Phys. **99**, 034503 (2006).
[7]N. Baguer and A. Bogaerts, J. Appl. Phys. **98**, 033303 (2005).
[8]U. Helmersson, M. Lattemann, J. Bohlmark, A. P. Ehiasarian, J. T. Gudmundsson, Thin Solid Films, **513**, 1 (2006).
[9]J. A. Hopwood, *Ionized Physical Vapor Deposition*, Thin Film Series Vol. 27, edited by J. A. Hopwood (Academic Press, San Diego, 2000).
[10]P. Ding, P. Gopalraja, J. Fu, J. Yu, Z. Xu, and F. Chen, Nanochip Technol. J. **1**, 47 (2005).
[11]J. Q. Lu, T. Yu, L. Stenzel, and J. Tobin, U.S. Patent No. 6471831 (29 October 2002).
[12]L. Meng, R. Raju, R. Flauta, H. Shin, D. N. Ruzic, and D. B. Hayden, J. Vac. Sci. Technol. A **28**, 112 (2009).
[13]K. Sarakinos, J. Alami, and S. Konstantinidis, Surf. Coat. Technol. **204**, 1661 (2010).
[14]L. Wu, E. Ko, A. Dulkin, K. J. Park, S. Fields, K. Leeser, L. Meng, and D. N. Ruzic, Rev. Sci. Instrum. **81**, 123502 (2010).